25th ABCM International Congress of Mechanical Engineering
October 20-25, 2019, Uberlândia, MG, Brazil

COB-2019-0239
EXPERIMENTAL ANALYSIS OF THE DYNAMIC RESPONSE OF A BEAM SUBJECTED TO A FLOW IN A WIND TUNNEL USING IMAGE PROCESSING METHOD

Jean César Hilário
Adailton Silva Borges
Rubens Gallo
Reynold Alves dos Santos
Universidade Tecnológica Federal do Paraná – Câmpus Cornélio Procópio
hilario@alunos.utfpr.edu.br, adailton@utfpr.edu.br, rubensgallo@utfpr.edu.br, reynold_alves@hotmail.com

Abstract. *The fluid-structure phenomenon has great impact on engineering areas, like civil with the air flow on buildings and aeronautic with flutter effect actuating during airplane flights. Thus, the development of applications in areas where this effect can occur are based on studies of results that could happen. This paper presents experimental analysis of a stainless-steel beam immersed in an air flow. The displacement profile is obtained by image processing techniques applied to the phenomenon record made with a low-cost high-speed digital camera. A natural frequency analysis was made from the displacement data to obtain the first natural frequency and using the Euler-Bernoulli beam theory the global force actuating in the structure was founded, making possible the determination of structure's drag coefficient. This result was compared with results from literature, founding a relative error of 1.95%, since the method applied to determine the drag coefficient attended to expectations. Future research is going to use numerical methods to compare the results and see the vibration modal shape, including the fluid-structures theory application to determine the key parameters of the phenomenon.*

Keywords: *Fluid-Structure Interactions, Image Processing, Vibration Analysis, Structural Dynamics.*

1. INTRODUCTION

The phenomenon produced by the interaction between fluid and structures can be found in many engineering fields, like civil, oceanic and aeronautic. This research presents the influence that the flow produces over the structure, being essential during the project development of products to avoid failures.

Structural vibrations produced by the flow comes from the vortex shedding. This phenomenon is based in the no-slip condition that affect the air that flows over the surface, where the particles velocity is reduced. Since the flow over the body keep constant, the particle tends to detach from the surface and start to flow. This air mass movement is responsible to change the pressure over the surface, resulting in vibrations. The present research relates the fluid-structure analysis of a structure (beam) submitted to an external flow in a wind tunnel where the displacement data are acquired with the processing of a set of images obtained with a digital camera.

The use of non-contact data acquisition method is of interest in the literature, since this does not change the boundary conditions of the problem under study (Giovannetti et al., 2016). The methods that have great focus are the Digital Image Correlation (Fedorov, 2012), Laser Doppler Vibrometer and High-Speed Cameras (Ducoin, Astolfi and Sigrist, 2012) and Particle Image Velocimetry (Giovannetti, 2016). Thus, the adopted method uses a high-speed camera without contact with the structure or the flow in order to capture the phenomenon without interference. The development of the algorithm used was omitted in the present work and more information can be found in (Baptista et al., 2016).

According to Rissá (2017), from the video analysis, it is possible to obtain the displacement profile of the structure under study through a frame-by-frame analysis of the digitized images of a video recorded by a digital camera. The data stored in the video are then processed numerically for image processing through Matlab® software. The last step is to perform the characterization of beam behavior at several points. The drag forces that excite the beam are calculated based on the linear beam theory of Euler Bernoulli (Leet, Uang and Gilbert, 2010).

The present study subject is to define the displacement profile and frequency of vibration caused in a structure by the mentioned phenomenon in order to begin the characterization of the parameters involved in the vortex shedding. The acquisition techniques are used mainly to do not influence the flow or the system properties, where the provided data was eligible to present good results once the processing is done using a precise algorithm.

2. METHODOLOGY

The proposed environment for flow generation was the wind tunnel of the Laboratory of Fluid Mechanics and Heat Transfer (LTCM) of the Federal University Technologic of Paraná, Department of Mechanical Engineering, Cornélio Procópio, PR. This equipment has the constructive characteristic of being open circuit type, as mentioned by Santos, Mesquita and Testezlaf (2013) there is no flow recirculation.

The flow is generated by an industrial fan OTAM LMS 355 ARR.4, with its speed of rotation being controlled by a frequency inverter. As speed control is given by the input frequency in the flow generator system, it is necessary to use a Pitot tube to determine the flow velocity in the test section, since this parameter appears squared in equations, its correct determination is of great importance.

To obtain the air speed of the wind tunnel flow the Eq. 1 provides a relation to use with a manometer (Tube U) and a Pitot tube. To realize the measurement, the Pitot tube is positioned in the test section of the wind tunnel as shown in Fig. 1, the industrial fan is turned on and after waiting 2 minutes (allow the flow to stabilize) the height difference on the manometer is recorded obtaining a value of 13 mm. Considering a gravitational acceleration of 9.8 m/s^2, the specific mass of air 1.2 kg/m^3 and of water 993.3 kg/m^3 (obtained experimentally from the measurements of mass and volume), a value of 14.5 m/s was obtained for the speed.

Figure 1. Experimental apparatus to obtain the flow's velocity.

$$V = (2g\Delta h(\rho_1/\rho_2))^{1/2} \quad (1)$$

where V is the air speed [m/s], g is the gravitational acceleration [m/s^2], Δh is the difference in height [m] between the two tubes in U tube manometer, ρ is the specific mass [kg/m^3] of work's fluid being the subscript 1 for air and 2 for water.

For the structural study, a beam model, produced in stainless steel, with dimensions of 210x24.4x0.46 mm was chosen with an elasticity's modulus of 193 GPa (Matweb, 2018).

Fig. 2a show the mechanical apparatus assembled in the wind tunnel, including the beam studied and the targets that enabled the characterization of the displacement through the image processing technique were identified. Fig. 2b show the targets identification number with the distance in millimeters from the base.

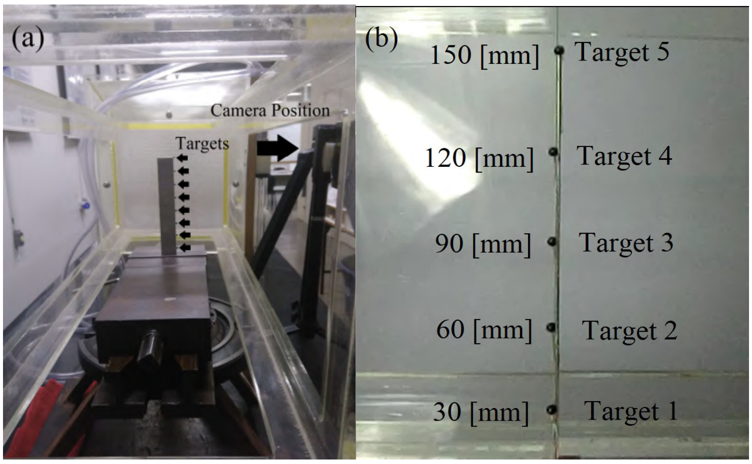

Figure 2. (a) Experimental apparatus utilized during the experiments, (b) Targets positioned at the beam with the respective distance from the fixed base.

Since the test section of the wind tunnel had an area of dimensions of 200x200 mm, the beam was fixed in such a way as to have a length of 150 mm enabling the air flow being in contact with all the beam front surface.

The targets had a spacing of 13 mm between them, in order to allow individual and joint identification, without interference. The analysis is done frame by frame recorded at a rate of 240 frames per second (FPS), a resolution of 432x320 pixels, a relation of millimeters/pixels of 0,3844 with a CASIO EXILIM EX-ZR100 digital camera during 20 seconds.

For the displacement profile to be obtained, the image processing technique will be performed according to Rissá (2017), which is performed by a code developed in MATLAB® referenced in Berton (2016) and in Baptista et al. (2016). The code identifies the targets in each frame of the record after a cut process in the image to exclude unnecessary information. The centroid definition is realized by the following operations: change the image to gray scale, subtraction of image color that is wanted from the general image followed by the thresholding that results in a binary image with only the target different from the background. This procedure makes possible find the intersection between two diagonals from the lesser rectangle inside the target. The algorithm then saves the position in pixel matrix and convert the unit from pixel to millimeter. When the software reaches the last frame, it prints the displacement-time graph and as an additional output the vibration frequency graph through the Fast Fourier Transform (FFT) of the displacement signal enabling the determination of the first natural frequency from the structure.

As one of the objectives is the experimental characterization of the drag coefficient, it is necessary to acquire the data that influence it. In the literature (Fox, McDonald and Pritchard, 2011), the coefficient of interest can be obtained by applying Eq. 2.

$$C_D = 2\,F_D/(\rho_1\,V^2\,A) \tag{2}$$

where C_D is the drag coefficient, F_D is the force acting in the front section of the body [N], A is the body front's area [m^2] that is in direct contact with the fluid during the flow.

The parameter to be determined is the acting force, because in the equation the area is determined by geometric characteristics, the velocity through the Pitot tube and the density of the air consulted in the literature. Due to the simplicity of the Euler-Bernoulli equations for beams, the consideration was made that the displacement would be governed by a linear behavior. This hypothesis will be evaluated by comparing the data obtained with the values presented in (Fox, McDonald and Pritchard, 2011), since the beam's shape chosen for the experiment is a common reference in this field of study.

The flow was considered as a distributed load throughout the structure, since the schematic is presented in Fig. 3. The deduction of Eq. 3 that will be used for force identification can be found in Bauchau and Craig (2009), along with their characteristics. Equation 4 follows the deduction made in Bauchau and Craig (2009), that present the displacement in any point of the beam can be estimated. The image processing of more points than only the fixed in the beam end was made and the results obtained was compared using Eq. 4 to prove if the Euler-Bernoulli equations are right for this kind of experiment.

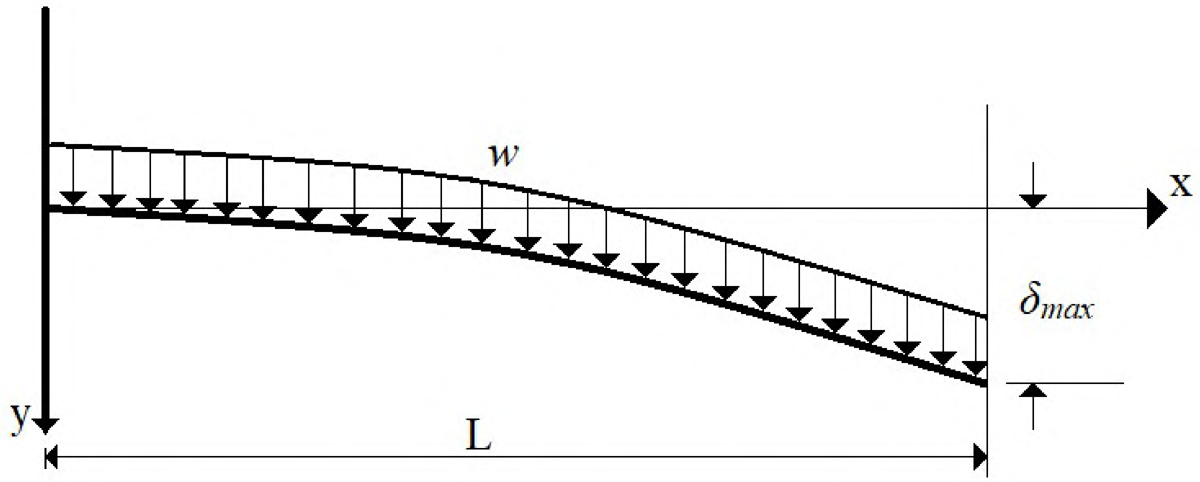

Figure 3. Cantilever beam with distributed load (Bauchau and Craig, 2009).

$$w = 8\,E\,I\,\delta_{max}/L^4 \tag{3}$$

$$y = ((w\,x^2)/(24\,E\,I))\,(x^2 + 6Ll^2 - 4\,L\,x) \tag{4}$$

where w is the uniform distributed load acting in the body [N/m], E is elasticity's modulus [Pa], I is the second moment of area [m^4], δ_{max} is the maximum deflection of the beam [m], L is the beam's total length [m], x is the coordinate [m] along the beam, y is the deflection [m] at any section in terms of x.

It should be noted that due to the shape of the structure, it is known that the drag force due to pressure for the present model is much larger than the drag force due to friction, leading the latter to be disregarded in this analysis. The default setting for tunnel vibration capture is to start recording the video after the steady flow rate has been reached. In order to determine the drag coefficient, the beam must be held in its initial position by means of an acrylic latch. The lock material was chosen so as not to interfere with the identification of the point of interest by the algorithm.

Therefore, the experimental configuration adopted was the fixation of the beam in its initial position, that is, without deformation, the motor of the wind tunnel is turned on and the waiting time was 30 seconds, so that the flow reached a permanent regime. At this point, the camera starts capturing images by video, after 2 seconds to identify the balance position, the latch is removed, and the beam is free for phenomena to occur.

The recording of the phenomenon was processed for 2 seconds, where the frequency of vibration caused by the vortex detachment and the displacement of the structure due to the pressure forces acting on the beam are identified. Further information regarding the determination of the displacements of a cantilever beam can be obtained in the work of (Rissá et al., 2016) and (Silvestre et al., 2016).

3. RESULTS

For the analysis of the phenomenon, the image processing took place in 480 of the frames that correspond to 2 seconds of capture of the phenomenon from the total recording. From the technique, displacement-time graphs can be obtained for previously identified targets of interest.

The theory considered for the calculation of the drag coefficient uses the point at the free end of the beam, thus it was isolated from the others during the displacement analysis for a greater efficiency in the data processing. Fig. 4 shows the plot of the displacement versus time for point "5" with the experimental configurations for the determination of displacement due to drag.

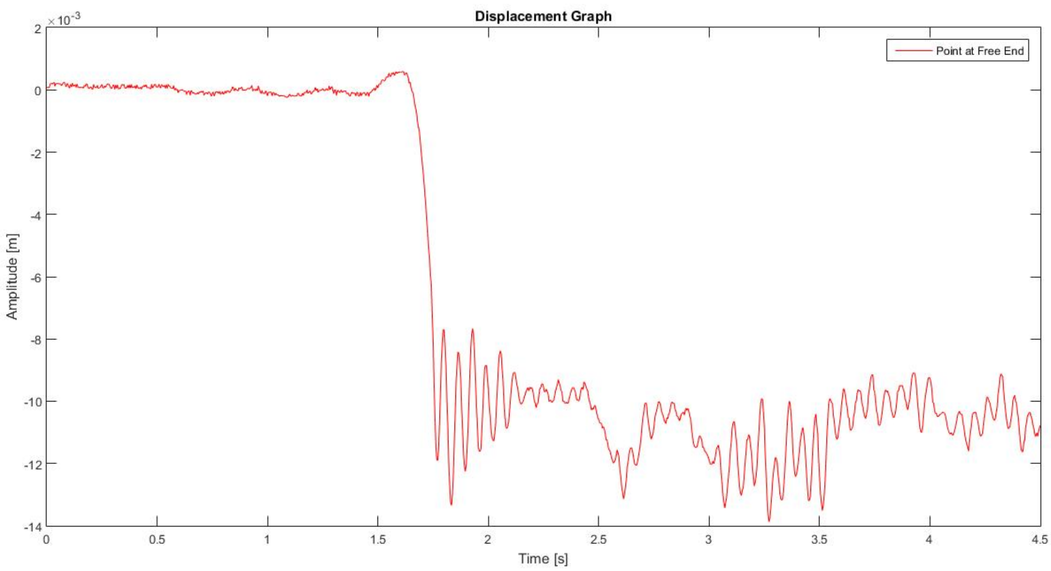

Figure 4. Displacement data obtained from experimental analysis for target 5.

In the graph obtained, two regions of interest are analyzed, the interval referring to the initial position of the point and the corresponding to the vibration of the structure after the displacement due to the forces of pressure. In Fig. 5 the regions mentioned above are observed.

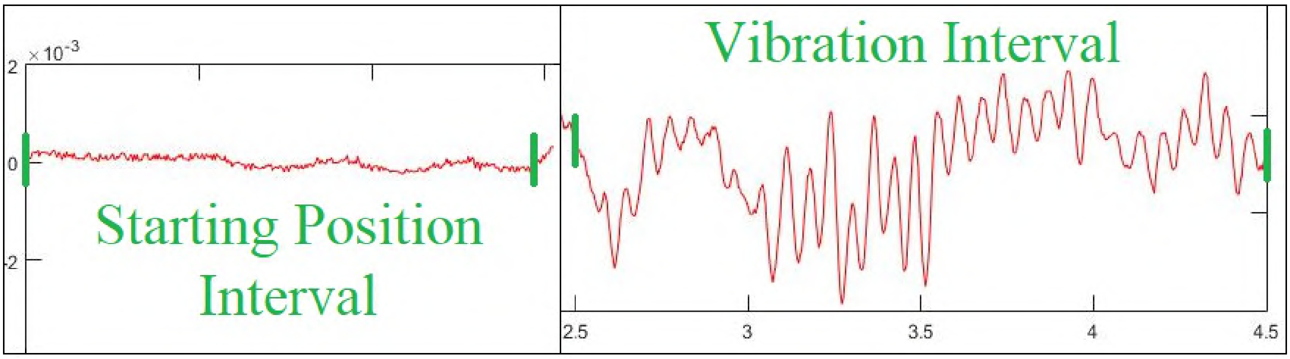

Figure 5. Displacement-time plot subdivided into intervals.

For these intervals a mean was calculated to identify the start point and the point caused by the displacement by pressure, with these values a displacement of 10.68 mm is obtained. Applying the Euler-Bernoulli equation for the type of structure studied, the distributed load found is 6.44 N/m. By the equation of the drag coefficient, we have that it has a value of 2.09. Comparing with the literature, for the boundary conditions the coefficient should be 2.05. Therefore, the relative error presented was 1.95%.

To analyze the Euler-Bernoulli beam theory adopted to find the load generated by the flow, the displacement in "y" direction of all targets was evaluated with the Matlab® algorithm and are shown in Table 1 with the displacement graphs for targets 2 to 5 presented in Fig. 6.

Table 1 – Experimental and theoretical displacement of target "5"

Target	Experimental Displacement [mm]	Theoretical Displacement [mm]	Difference in Displacement [mm]
5	10.68	10.68	0

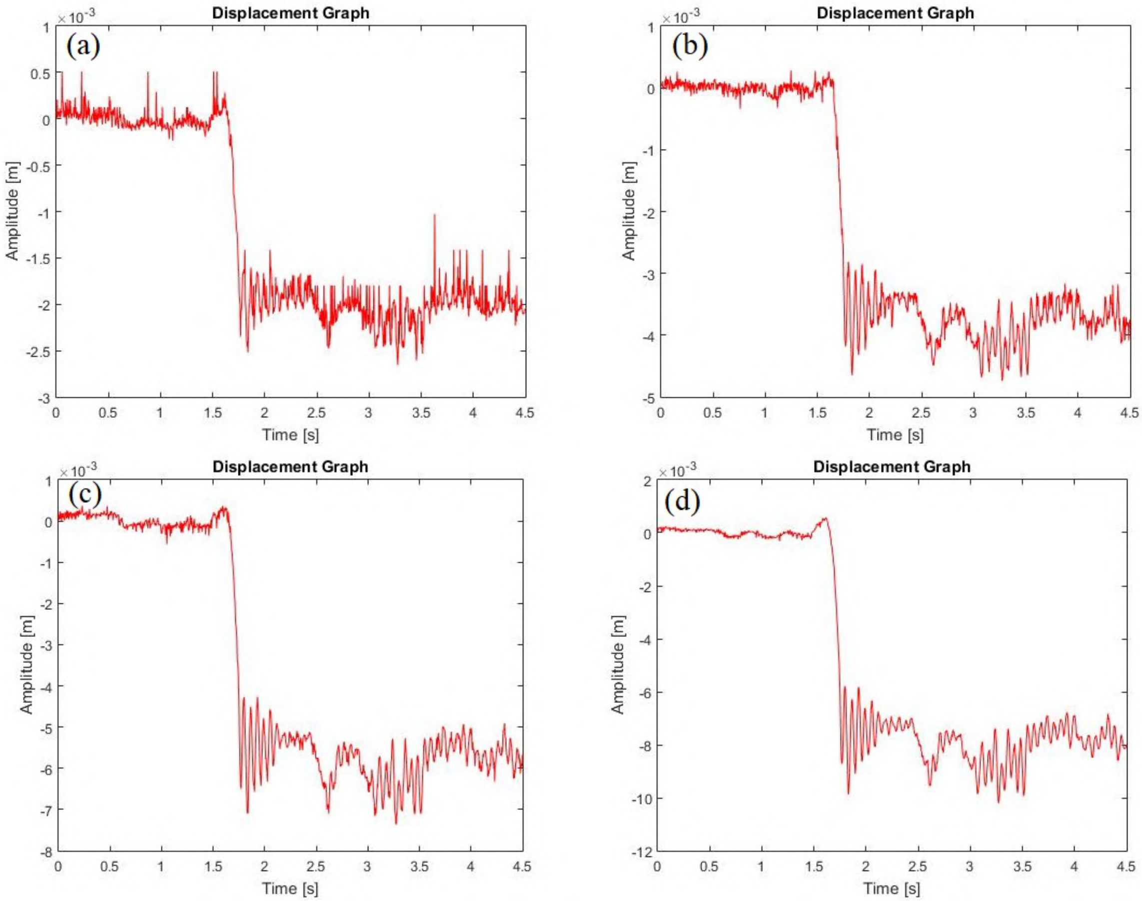

Figure 6. Displacement data obtained from experimental analysis for target 1 (Fig. a), 2 (Fig. b), 3 (Fig. c) and 4 (Fig. d).

For the vibration analysis, the interval after the stabilization of the position due to the pressure forces was considered. In this signal of displacement, the Fast Fourier Transform (FFT) was applied in order to identify the vibration frequency, where the graph of the frequency shift is shown in Fig. 7 for the free end, where the peak was 15.97 Hz and the same result is obtained as presented in Fig. 8.

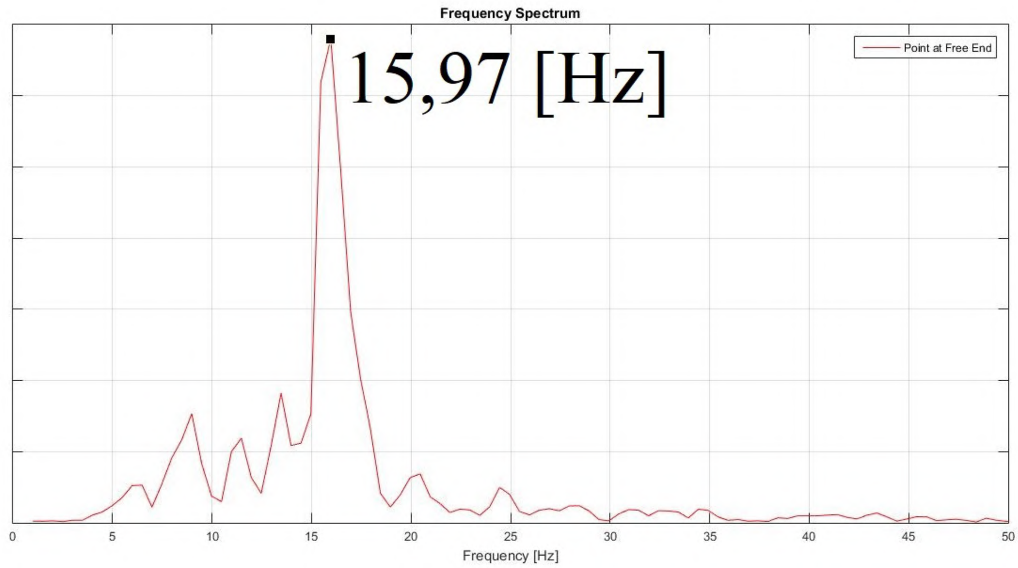

Figure 7. Displacement graph for the free end, target "5" obtained in the frequency domain by FFT.

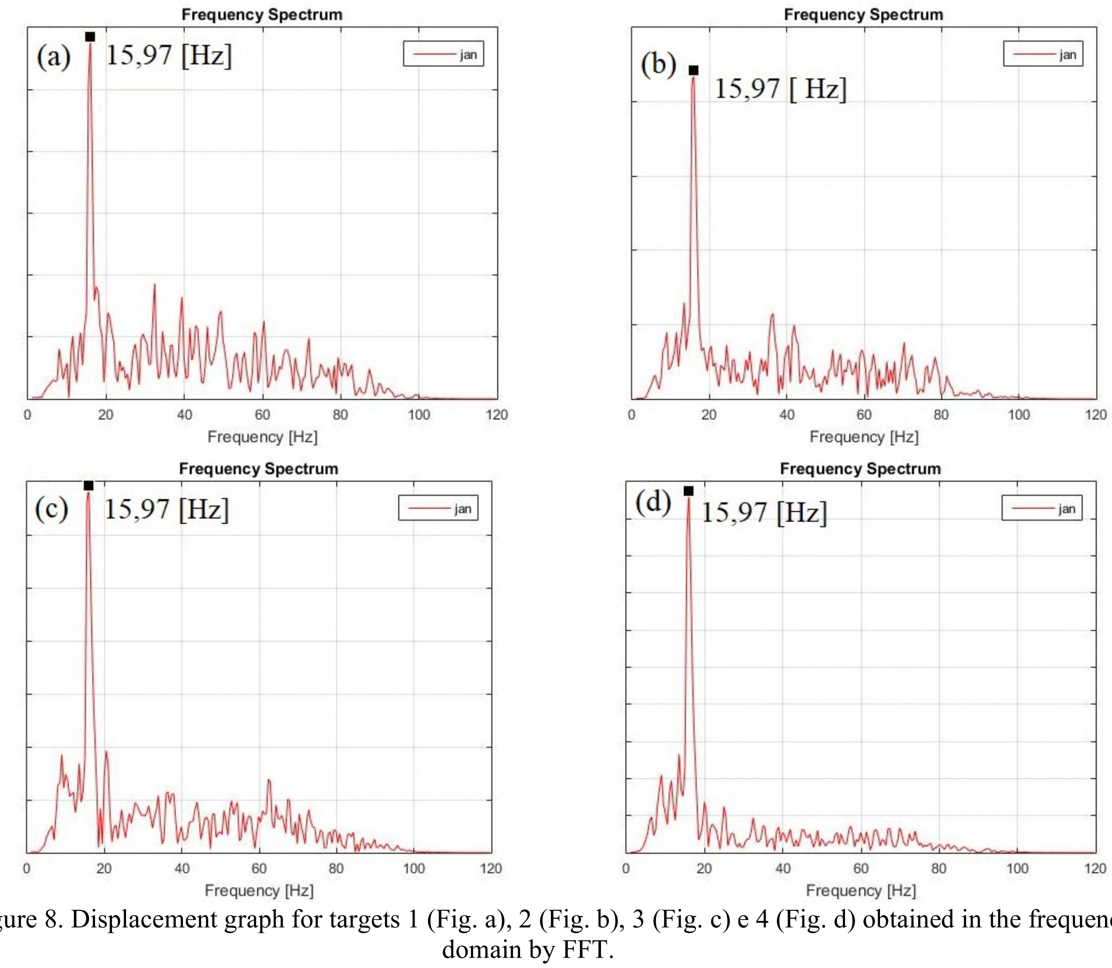

Figure 8. Displacement graph for targets 1 (Fig. a), 2 (Fig. b), 3 (Fig. c) e 4 (Fig. d) obtained in the frequency domain by FFT.

4. CONCLUSIONS

The present work presented the results obtained for the displacement and frequency of vibration of a beam immersed in a flow. From the data obtained, it was concluded that the method for identifying the target presented qualitatively satisfactory results, showing the displacement caused by the drag force and the vibration due to the vortex detachment as expected by the authors. The noise found on the frequency's graph is related with the relation millimeter-pixel and the displacement's amplitude of each point, where a low amplitude results in a higher noise.

The linear theory used to calculate the drag coefficient influences the result and can be the cause of the relative errors presented where the difference between the experimental and theoretical displacements over the beam was shown to prove the need to use another approach, since the beam displacement is above the limit established by the literature, therefore, future experiments will be carried out using nonlinear theories to compare the approximation performed.

From the graph analyzed in the frequency domain, it is known that only the first natural frequency was identified, in this way, future analyzes will be made with the objective of identifying the natural frequencies of the structure and using specific theories for the phenomenon of vortex detachment, in order to characterize the experiment completely.

5. ACKNOWLEDGEMENTS

The authors would like to acknowledge the teams of the Laboratories of Heat Transfer and Fluid Mechanics and the Technological of Mechanical Vibrations and Maintenance and Universidade Tecnológica Federal do Paraná – Cornélio Procópio for the support provided to the research.

6. REFERENCES

Baptista, R. G., Silvestre, T., Santos, F. H. T., Takahama, M. H. And Borges, A. S., 2016. Medição de deslocamento com auxílio de uma câmera de alta velocidade como sensor sem contato. *VI Simpósio Paranaense de Engenharia Mecânica.*

Bauchau, O. A. And Craig, J. I., 2009. Structural Analysis with Applications to Aerospace Structures. *Solid Mechanics and its Applications - Springer.*

Berton Junior, J. 2016. *Medidas de deslocamento em 2D e 3D utilizando câmera digital como sensor sem contato.* Master thesis, Universidade Tecnológica Federal do Paraná, Cornélio Procópio, Paraná, Brasil.

Ducoin, A., Astolfi, J, A., Sigrist, J. F., 2012. An experimental analysis of fluid structure interaction on a flexible hydrofoil in various flow regimes including cavitating flow. *Eur. J. Mech. B/Fluids,* Vol. 36, pp. 63-74.

Fedorov, V., 2012. *Bend-Twist Coupling Effects in Wind Turbine Blades*. Ph.D. thesis, Technical University of Denmark.

Fox, R.W., McDonald, A.T. and Pritchard, P.J.; 2011. *Introduction to Fluid Mechanics*, LTC, 8th edition.

Giovannetti, L. M., Banks, J., Turnock, S. R., 2017. Uncertainty assessment of coupled Digital Image Correlation and Particle Image Velocimetry for fluid-structure interaction wind tunnel experiments. *Journal of Fluids and Structures*, Vol 68, pp. 125-140.

Leet, K. M., Uang, C. Gilbert, A. M., 2010. *Fundamentos da Análise Estrutural.* Amgh, Porto Alegre:, 3rd edition.

MATWEB. "304 Stainless Steel". Material Property Data. 30 Mar. 2018 <http://www.matweb.com/search/DataSheet.aspx?MatGUID=abc4415b0f8b490387e3c922237098da&ckck=1>.

Rissá, H. S., Takahama, M. H., Tanaka, F. H., Borges, A. S., 2016. Identificação de deslocamentos por meio da utilização de uma câmera digital como sensor sem contato. *18º Congresso de Tecnologia*, Faculdade de Tecnologia, São Paulo, Brasil.

Rissá, H. S., 2017. *Identificação de deslocamentos de baixa amplitude e frequência utilizando uma câmera digital.* Master thesis. Universidade Tecnológica Federal do Paraná, Cornélio Procópio, Paraná, Brasil.

Santos, M. B., Mesquita, M., Testezlaf, R. Aplicação de tunél de vento na avaliação de linahs de fluxo geradas por crepinas de filtros de areia. *Artigo Técnico, Eng. Agríc.,* Jaboticabal, Vol. 33, N. 3, pp. 548-559, Mai/Jun. 2013.

Silvestre, T., Baptista, R. G., Tanaka, F. H., Takahama, M. H., Borges, A. S., 2016. Medida de deslocamento utilizando uma câmera de alta velocidade como sensor sem contato. *18º Congresso de Tecnologia*, Faculdade de Tecnologia, São Paulo, Brasil.

7. RESPONSIBILITY NOTICE

The authors are the only responsible for the printed material included in this paper.